

Improved Resummation Prediction on Higgs Production at Hadron Colliders

Jian Wang,¹ Chong Sheng Li,^{1,2,*} Zhao Li,^{3,†} C.-P. Yuan,^{3,2,‡} and Hai Tao Li¹

¹*Department of Physics and State Key Laboratory of Nuclear Physics and Technology, Peking University, Beijing 100871, China*

²*Center for High Energy Physics, Peking University, Beijing 100871, China*

³*Department of Physics & Astronomy, Michigan State University, E. Lansing, MI 48824, USA*

We improve the resummation formula in ResBos for Higgs boson production by including NNLO Wilson coefficient functions and G-functions, which leads to increasing the total cross section prediction of ResBos for Higgs production by about 8% at the Tevatron and about 6% at the LHC. The HNNLO predictions at NNLO and the HqT predictions with NNLL+NLO accuracy are consistent with our results, i.e. the improved ResBos prediction, within a couple of percent for total Higgs production cross sections at both the Tevatron and LHC. For the transverse momentum distribution, the improved predictions of ResBos generally increase the overall size of the distribution. Especially, the improvement in the small transverse momentum region can be as large as 20% at both the Tevatron and LHC, but the peak position is not changed. The HqT predictions for the transverse momentum distribution at the LHC are almost the same as the improved ResBos, except that at the Tevatron the peak height of the HqT prediction is a little lower than that of the improved ResBos by about 2%. The G-functions can only modify the shape of transverse momentum distribution within 1%. Besides, we investigate the dependence of the transverse momentum distribution for Higgs production on the non-perturbative coefficients, which can slightly change the peak position and height of the distribution.

PACS numbers: 12.38.Cy,12.38.Qk,14.80.Bn

I. INTRODUCTION

The Higgs boson is the last missing particle for the Standard Model (SM), and it is responsible for the origin of the electroweak symmetry spontaneous breaking and elementary particle masses in the SM. In the past decades the Fermilab Tevatron has devoted great effort to searching for Higgs boson in the SM or new physics models. Although there is still no definite evidence for the discovery of Higgs boson, the Tevatron has excluded a wide range of the Higgs boson mass. Recently with up to 10 fb^{-1} luminosity data the combined analysis by CDF and $D\bar{0}$ collaborations found about 2σ excess in the mass region $115 \text{ GeV} < m_H < 135 \text{ GeV}$ [1]. Meanwhile at the CERN Large Hadron Collider (LHC) the ATLAS [2] and CMS [3] analyses for an integrated luminosity of about 4.9 fb^{-1} have found about 3σ excess for the Higgs mass in the range $124 \text{ GeV} < m_H < 126 \text{ GeV}$. Within one more year running on 8 TeV center-of-mass (CM) energy, it is promising that LHC can exclude or discover the SM Higgs boson.

The main Higgs production mechanism at the LHC is the gluon fusion process. At the lowest order the Higgs boson couples with gluon via top quark loop, and the higher order corrections will involve multi-loop diagrams. The QCD next-to-leading order (NLO) corrections to this process have been computed both in the limit of infinite top quark mass [4, 5] and for finite top quark mass [6, 7], which enhance the total cross section by more than 80% at the LHC. The QCD next-to-next-to-leading order (NNLO) result for the inclusive total cross section is calculated in the infinite top quark mass limit [8–10], increasing the NLO cross result by about 25%. The validity of this limit at NNLO has been justified in Refs.[11–13]. The soft-gluon contributions have been resummed up to next-to-next-to-leading logarithm (NNLL) [14], leading to an additional increase of the cross section of about 7%. Recently, in addition to the soft-gluon resummation at next-to-next-to-next-to-leading logarithm (NNNLL), the contributions in the form of $(C_A \pi \alpha_s)^2$ have been considered in the soft-collinear effective theory [15, 16]. An precise prediction of the transverse momentum distribution of the Higgs boson is of crucial importance to discover the SM Higgs, which has been calculated at QCD NLO [17–21] and NNLO [22]. Also, recently the logarithmically-enhanced contributions due to soft-gluon emission have been computed at NNLL [23–27].

In the further Higgs investigation it is significant to achieve higher accuracy and better reliability for the theoretical prediction, which is very sensitive to the high order QCD effect including fixed order correction and resummation effect. Besides, due to the fact that for soft gluon resummation effect the values of non-perturbative coefficients

*Electronic address: csli@pku.edu.cn

†Electronic address: zhaoli@pa.msu.edu

‡Electronic address: yuan@pa.msu.edu

are obtained by fitting the experiment data of Drell-Yan processes with quark initial states, the non-perturbative coefficients for $gg \rightarrow H$ are scaled by color factor ratio C_A/C_F . However, the non-perturbative physics may not follow this assumption, so when we provide the soft gluon resummation prediction on $gg \rightarrow H$ the theoretical uncertainty from the dependence on non-perturbative coefficients is also investigated.

In this paper, we show the improvement on the transverse momentum resummation formula in ResBos [28], in which the large logarithms of the form $\ln^n(m_H^2/Q_T^2)$ have been resummed to all orders in α_s . The improved ResBos includes the Wilson coefficient function up to NNLO and the Sudakov exponent with NNLL accuracy, and matches to the $\mathcal{O}(\alpha_s^4)$ fixed order prediction at large transverse momentum region. Then we compare the improved resummation prediction for the total cross section and transverse momentum distribution with those from the parton level Monte Carlo programs HNNLO [20, 21] and HqT [23–26]. The HqT prediction includes resummation coefficients up to NNLL order matched to NLO at large transverse momentum region, and its normalization is the NNLO total cross section.

This paper is organized as follows. In Sec. II, we briefly review the formula of transverse momentum resummation for Higgs boson production, and the explicit expressions of NNLO Wilson coefficient functions are shown. In Sec. III, we present the numerical results for the total cross section and transverse momentum distribution given by the improved ResBos, and compare them with the HNNLO and HqT predictions. Conclusion is made in Sec. IV.

II. RESUMMATION FORMULA

In this section we briefly review the Collins-Soper-Sterman (CSS) [29–31] formula of the soft gluon resummation for Higgs production and decay [32] used in ResBos [28]. By using the narrow width approximation the Higgs production can be factorized from its subsequent decay. The resummation formula for inclusive differential cross section for $gg \rightarrow H$ can be written as [32, 33]

$$\frac{d\sigma(gg \rightarrow HX)}{dQ^2 dQ_T^2 dy} = \kappa \sigma_0 \frac{Q^2}{S} \frac{Q^2 \Gamma_H / m_H}{(Q^2 - m_H^2)^2 + (Q^2 \Gamma_H / m_H)^2} \times \left\{ \frac{1}{(2\pi)^2} \int d^2 b e^{iQ_T \cdot b} \widetilde{W}_{gg}(b_*, Q, x_1, x_2, C_{1,2,3}) \widetilde{W}_{gg}^{NP}(b, Q, x_1, x_2) + Y(Q_T, Q, x_1, x_2, C_4) \right\}, \quad (1)$$

where S is the square of the CM energy; Q , Q_T , y , and Γ_H are the invariant mass, transverse momentum, rapidity, and total decay width of the Higgs boson, respectively, defined in the lab frame. In Eq. (1), the quantity

$$\sigma_0 = \frac{\sqrt{2} G_F \alpha_s^2}{576\pi}, \quad (2)$$

arises as an overall factor in the infinite top quark mass limit, where α_s is evaluated at the hard scale $C_2 Q$ with $C_2 = 1$ being the canonical value. Furthermore, we have multiplied $\sigma^{\text{LO}}(\infty, 0, 0)$ by an additional factor

$$\kappa = \frac{\sigma^{\text{LO}}(m_t, m_b, m_c)}{\sigma^{\text{LO}}(\infty, 0, 0)}, \quad (3)$$

which takes into account the masses of the top, bottom, and charm quarks at LO. It has been shown that multiplying the NLO Higgs cross section in the infinite top quark mass limit by the factor κ is a good approximation to the full mass-dependent NLO cross section over a wide range of the Higgs boson mass [34]. The total cross section can be obtained by integrating the result in Eq. (1) over the transverse momentum and rapidity.

In Eq.(1), the term containing \widetilde{W}_{gg} dominates at small Q_T , growing as Q_T^{-2} times a resummation in powers of $\ln Q^2/Q_T^2$, to all orders in α_s . It can be expressed as

$$\widetilde{W}_{gg}(b, Q, x_1, x_2, C_{1,2,3}) = e^{-S(b, Q, C_1, C_2)} \sum_{a,b} (C_{ga} \otimes f_a)(x_1) (C_{gb} \otimes f_b)(x_2), \quad (4)$$

where the Sudakov exponent is given by

$$S(b, Q, C_1, C_2) = \int_{C_1^2/b^2}^{C_2^2 Q^2} \frac{d\bar{\mu}}{\bar{\mu}^2} \left[A(\alpha_s(\bar{\mu}), C_1) \ln \left(\frac{C_2^2 Q^2}{\bar{\mu}^2} \right) + B(\alpha_s(\bar{\mu}), C_1, C_2) \right]. \quad (5)$$

The coefficients A and B and the Wilson coefficient functions C_{ga} can be expanded as a power series in α_s :

$$A(\alpha_s(\bar{\mu}), C_1) = \sum_{n=1}^{\infty} \left(\frac{\alpha_s(\bar{\mu})}{\pi} \right)^n A^{(n)}(C_1), \quad (6)$$

$$B(\alpha_s(\bar{\mu}), C_1, C_2) = \sum_{n=1}^{\infty} \left(\frac{\alpha_s(\bar{\mu})}{\pi} \right)^n B^{(n)}(C_1, C_2), \quad (7)$$

and

$$C_{ga}(x, b, \mu, C_1, C_2) = \sum_{n=0}^{\infty} \left(\frac{\alpha_s(\mu)}{\pi} \right)^n C_{ga}^{(n)}(z, b, \mu, \frac{C_1}{C_2}), \quad (8)$$

with $\mu = C_3/b$. These quantities can be extracted order-by-order from the fixed-order calculations. In the old version of ResBos, we have included $A^{(1,2,3)}$, $B^{(1,2)}$ and $C^{(0,1)}$, whose analytical expressions are given in Ref.[32]. We use the canonical choice for the renormalization constants, $C_1 = C_3 = b_0 = 2e^{-\gamma_E}$, $C_2 = C_4 = 1$, which simplifies the above expressions. The function \tilde{W}_{gg}^{NP} describes the non-perturbative part of the soft-gluon resummation, in which we use the BLNY parameterization [35], but with the nonperturbative coefficients $g_{1,2,3}$ scaled by the factor $C_A/C_F = 9/4$. This scaling factor is to recognize that the initial state partons are gluons in the $gg \rightarrow H$ process, in contrast to quarks in the Drell-Yan process. The term containing Y incorporates the remainder of the cross section, which is not singular as $Q_T \rightarrow 0$, as explained in Ref. [32].

In this paper, we improve ResBos by including the NNLO Wilson coefficient functions

$$\begin{aligned} C_{gg}^{(2)} = & C_A C_F \left\{ \text{Li}_2(z) \left[\frac{z^2}{3} - \frac{z}{2} - \frac{11}{6z} + \left(\frac{3z}{4} + \frac{3}{2z} - \frac{1}{2} \right) \ln(z) + 2 \right] - \frac{3[(z+1)^2+1]}{4z} \text{Li}_3(-z) \right. \\ & + \left(-\frac{5z}{4} - \frac{5}{2z} + \frac{1}{2} \right) \text{Li}_3(z) - \frac{[(1+z)^2+1]}{2z} \text{Li}_3\left(\frac{1}{z+1}\right) + \text{Li}_2(-z) \left(\frac{z}{4} + \frac{(1+z)^2+1}{4z} \ln(z) \right) \\ & + \left(\frac{38}{27} - \frac{\pi^2}{18} \right) z^2 + \frac{-5z^2 - 22(1-z) + 6[(1-z)^2+1] \ln(z)}{48z} \ln^2(1-z) + \frac{1}{48} (8z^2 + 9z + 36) \ln^2(z) \\ & + \frac{[(1+z)^2+1] [3\ln^2(z) - \pi^2] - 6z^2 \ln(z)}{24z} \ln(1+z) + \left(-\frac{11z^2}{9} + \frac{z}{12} - \frac{1}{z} - \frac{107}{24} \right) \ln(z) \\ & + \frac{-43z^2 + 6(4z^3 - 9z^2 + 24z - 22) \ln(z) + 152z + 9[(1-z)^2+1] \ln^2(z) - 152}{72z} \ln(1-z) \\ & + \frac{1}{z} \left(4\zeta(3) - \frac{503}{54} + \frac{11\pi^2}{36} \right) + z \left(2\zeta(3) - \frac{133}{108} + \frac{\pi^2}{3} \right) - \frac{(1-z)^2+1}{24z} \ln^3(1-z) - \frac{1}{12} \left(\frac{z}{2} + 1 \right) \ln^3(z) \\ & + \frac{(1+z)^2+1}{12z} \ln^3(z+1) - \frac{5\zeta_3}{2} - \frac{\pi^2}{3} + \frac{1007}{108} \left. \right\} - \frac{C_F z}{8} [(5+\pi^2) C_A - 3C_F] + C_A C_F \frac{2(1-z) + (z+1) \ln(z)}{z} \\ & + C_F^2 \left\{ -\frac{13z}{16} + \frac{1}{12} \left(\frac{z}{2} + \frac{1}{z} - 1 \right) \ln^3(1-z) + \frac{1}{48} (2-z) \ln^3(z) + \frac{1}{16} \left(z + \frac{6}{z} - 6 \right) \ln^2(1-z) \right. \\ & \left. - \frac{1}{32} (3z+4) \ln^2(z) + \left(\frac{5z}{8} + \frac{2}{z} - 2 \right) \ln(1-z) + \frac{5}{16} (z-3) \ln(z) + \frac{5}{8} \right\} \\ & + C_F n_f \left\{ \frac{13z}{108} + \frac{14}{27z} + \frac{(1-z)^2+1}{24z} \ln^2(1-z) + \frac{1}{18} \left(z + \frac{5}{z} - 5 \right) \ln(1-z) - \frac{14}{27} \right\} \\ & - \frac{(z^2+2z+2) \ln(z) - 2z^2}{z} \ln(z) \ln(1+z), \end{aligned} \quad (9)$$

and

$$\begin{aligned} 2C_{gg}^{(2)} = & \delta(z-1) \left\{ C_A^2 \left[\frac{7}{8} \ln\left(\frac{m_H^2}{m_t^2}\right) - \frac{55\zeta_3}{18} + \frac{13\pi^4}{144} + \frac{157\pi^2}{72} + \frac{3187}{288} \right] + C_A C_F \left[-\frac{11}{8} \ln\left(\frac{m_H^2}{m_t^2}\right) - \frac{3\pi^2}{4} - \frac{145}{24} \right] \right. \\ & \left. - C_A n_f \left(\frac{4\zeta_3}{9} + \frac{287}{144} + \frac{5\pi^2}{36} \right) - \frac{5C_A}{96} + \frac{9C_F^2}{4} + C_F n_f \left[\frac{1}{2} \ln\left(\frac{m_H^2}{m_t^2}\right) + \zeta_3 - \frac{41}{24} \right] - \frac{C_F}{12} \right\} \end{aligned}$$

$$\begin{aligned}
& + C_A^2 \left\{ \frac{(1-z)(11z^2-z+11)}{3z} \text{Li}_2(1-z) + \frac{(z^2+z+1)^2}{z(z+1)} \left[2\text{Li}_3\left(\frac{z}{z+1}\right) - \text{Li}_3(-z) \right] \right. \\
& + \frac{(z^2+z+1)^2}{z(z+1)} \left[\text{Li}_2(-z) \ln(z) - \frac{1}{3} \ln^3(z+1) + \frac{1}{6} \pi^2 \ln(z+1) \right] - \frac{z^5-5z^4+z^3+5z^2-z+5}{z(1-z^2)} [\text{Li}_3(z) - \zeta_3] \\
& + \frac{z^5-3z^4+z^3+3z^2-z+3}{z(1-z^2)} \text{Li}_2(z) \ln(z) + \frac{835z^2}{54} - \frac{(-z^2+z+1)^2}{6(1-z^2)} \ln^3(z) \\
& + \left[\frac{1}{24} (44z^2-11z+25) + \frac{(z^2-z+1)^2}{2z(1-z)} \ln(1-z) - \frac{(z^2+z+1)^2}{2z(1+z)} \ln(1+z) \right] \ln^2(z) \\
& + \left[\frac{(z^2-z+1)^2}{2z(1-z)} \ln^2(1-z) + \frac{(z^2+z+1)^2}{z(1+z)} \ln^2(1+z) + \frac{-536z^3-149z^2-773z-72}{72z} \right] \ln(z) + \\
& \left. \frac{(-12z^4-10z^3-22z^2-17z+2)\zeta(3)}{2z(z+1)} - \frac{380z}{27} - \frac{449}{27z} + \frac{1}{12} z \log(1-z) + \frac{517}{27} \right\} \\
& + C_A^2 \frac{-2z+(z+1)\ln(z)+2}{z} - \frac{1}{16} [(5+\pi^2)C_A-3C_F]^2 \delta(1-z) + \left(\frac{1}{1-z} \right)_+ \left[C_A^2 \left(\frac{7\zeta_3}{2} - \frac{101}{27} \right) + \frac{14C_A n_f}{27} \right] \\
& + C_A n_f \left[-\frac{139z^2}{108} + \frac{55z}{54} + \frac{121}{108z} + \frac{1+z}{12} \ln^2(z) - \frac{1}{12} z \ln(1-z) + \frac{10z+13}{36} \ln(z) - \frac{83}{54} \right] \\
& + C_F n_f \left[-\frac{(1-z)(z^2-23z+1)}{6z} + \frac{1+z}{12} \ln^3(z) + \frac{3+z}{8} \ln^2(z) + \frac{3}{2}(z+1)\ln(z) \right]. \tag{10}
\end{aligned}$$

The above coefficients are obtained by the equation [36]

$$\begin{aligned}
\int_0^{Q_0^2} dq_T^2 \frac{d\hat{\sigma}_{ab \rightarrow H}}{dq_T^2}(q_T, m_H, \hat{s}) & \equiv \int_0^{+\infty} dq_T^2 \frac{d\hat{\sigma}_{ab \rightarrow H}}{dq_T^2}(q_T, m_H, \hat{s}) - \int_{Q_0^2}^{+\infty} dq_T^2 \frac{d\hat{\sigma}_{ab \rightarrow H}}{dq_T^2}(q_T, m_H, \hat{s}) \\
& = \hat{\sigma}_{ab \rightarrow H}^{(\text{tot})}(m_H, \hat{s}) - \int_{Q_0^2}^{\infty} dq_T^2 \int_{-\infty}^{+\infty} d\hat{y} \frac{d\hat{\sigma}_{ab \rightarrow H}}{d\hat{y} dq_T^2}(\hat{y}, q_T, m_H, \hat{s}), \tag{11}
\end{aligned}$$

where $\hat{\sigma}_{ab \rightarrow H}$ is the partonic cross section of Higgs boson production process $ab \rightarrow H$ and Q_0 is a small transverse momentum cut. The left hand side of Eq.(11) can be expressed as

$$\int_0^{Q_0^2} dq_T^2 \frac{d\hat{\sigma}_{ab \rightarrow H}}{dq_T^2}(q_T, m_H, \hat{s} = m_H^2/z) \equiv z \sigma_0 \hat{R}_{ab \rightarrow H}(z, m_H/Q_0), \tag{12}$$

in which σ_0 is the Born level partonic cross section in Eq.(2) and

$$\begin{aligned}
\hat{R}_{ab \rightarrow H}^{(2)}(z, m_H/Q_0) & = l_0^4 \Sigma_{gg \leftarrow ab}^{H(2;4)}(z) + l_0^3 \Sigma_{gg \leftarrow ab}^{H(2;3)}(z) + l_0^2 \Sigma_{gg \leftarrow ab}^{H(2;2)}(z) + l_0 \left(\Sigma_{gg \leftarrow ab}^{H(2;1)}(z) - 16\zeta_3 \Sigma_{gg \leftarrow ab}^{H(2;4)}(z) \right) \\
& + \left(\mathcal{H}_{gg \leftarrow ab}^{H(2)}(z) - 4\zeta_3 \Sigma_{gg \leftarrow ab}^{H(2;3)}(z) \right) + \mathcal{O}(Q_0^2/m_H^2), \tag{13}
\end{aligned}$$

with $l_0 = \log[m_H^2/Q_0^2]$ and $\Sigma_{gg \leftarrow ab}^{H(2;n)}$, $n = 1, \dots, 4$ are known in the transverse momentum resummation scheme. In the limit $Q_0 \rightarrow 0$, the terms $\mathcal{O}(Q_0^2/m_H^2)$ can be neglected. Here,

$$\mathcal{H}_{gg \leftarrow ab}^{H(2)}(z) = \delta_{ga} C_{gb}^{(2)}(z) + \delta_{gb} C_{ga}^{(2)}(z) + C_{ga}^{(1)} \otimes C_{gb}^{(1)}(z) + G_{ga}^{(1)} \otimes G_{gb}^{(1)}(z), \tag{14}$$

and it can be found in the code HNNLO [20, 21]. We have numerically checked Eq.(11) using the analytical expressions for the total cross section in Ref.[9] and transverse momentum distribution in Ref. [18].

The function $\widetilde{W}_{gg}^{N\!P}$ describes the non-perturbative part of the soft-gluon resummation, where we use the BLNY parameterization [35], but with the nonperturbative coefficients $g_{1,2,3}$ scaled by the factor $C_A/C_F = 9/4$. This scaling factor is to recognize that the initial state partons are gluons in the $gg \rightarrow H$ process, in contrast to quarks in the Drell-Yan process.

Besides, the G-function can be included into the traditional CSS formula as shown in Ref. [36]. Therefore, the resummed function \widetilde{W} can be further improved as

$$\widetilde{W}_{gg}(b, Q, x_1, x_2, C_{1,2,3}) = e^{-S(b, Q, C_1, C_2)} \sum_{a,b} [(C_{ga} \otimes f_a)(x_1)(C_{gb} \otimes f_b)(x_2) + (G_{ga} \otimes f_a)(x_1)(G_{gb} \otimes f_b)(x_2)]. \quad (15)$$

The lowest order of G-function is at $\mathcal{O}(\alpha_s/\pi)$

$$G_{ga}(z, \alpha_s) = \frac{\alpha_s}{\pi} G_{ga}^{(1)}(z) + \sum_{n=2}^{\infty} \left(\frac{\alpha_s}{\pi}\right)^n G_{ga}^{(n)}(z). \quad (16)$$

where the coefficient functions are known [36, 37]

$$G_{gg}^{(1)} = C_A \frac{1-z}{z}, \quad G_{gq}^{(1)}(z) = C_F \frac{1-z}{z}. \quad (17)$$

Finally, in Eq.(1), the term containing Y incorporates the remainder of the cross section, which is not singular as $Q_T \rightarrow 0$. It consists of the difference between the full cross section at finite Q_T and the small- Q_T limit of this cross section, each calculated to the same order in α_s . At small Q_T , these cancel with each other, so that the contribution of the Y -term is small, and the resummed term dominates. At large Q_T , where the logarithms become small, the resummed term cancels against the small- Q_T limit term (to the given order in α_s), so that the cross section approaches to the fixed-order calculation. More details of how this matching process between the resummed calculation and the fixed-order one is implemented in ResBos can be found in Ref. [28].

III. NUMERICAL RESULTS

In this section we investigate the effect on the total cross section and transverse momentum distribution by including the NNLO Wilson coefficient function and G-function contributions. The parton distribution function (PDF) is chosen as CTEQ6.6 [38]. The total cross sections and transverse momentum distributions for the Higgs boson production are presented for different scale choices by varying C_2 around the canonical choice ($C_2 = 1$) by a factor of two, but with the relations

$$C_1 = C_2 b_0, \quad C_3 = b_0 \quad \text{and} \quad C_4 = C_2. \quad (18)$$

Keeping the relations between C_i , the Wilson coefficient functions are not changed. Therefore, the dominant effect of the variation is to change the shape, but not the overall size of the cross section. Also we present the NNLO prediction on the total cross section from HNNLO [20, 21] and NNLL+NLO prediction on the transverse momentum distribution from HqT [23, 24, 26] to compare with the improved ResBos prediction.

TABLE I shows the different theoretical predictions of the total cross sections for Higgs boson production at the Tevatron and LHC. By including the NNLO Wilson coefficient function $C^{(2)}$ the improved ResBos predictions at Tevatron and LHC 7 TeV (8 TeV, 14 TeV) increase the resummation theoretical results by about 8% and 6% (9%, 6%), and the different scale choices present the theoretical uncertainties in the resummation formula reduced to about 9% and 8% (7%, 8%), compared with the result only including $C^{(1)}$ and are smaller than those of HNNLO and HqT predictions. The NNLO predictions from HNNLO and the NNLL+NLO predictions from HqT agree with ResBos within a couple of percent. Notice that when the CM energy of the LHC increased from 7 TeV to 8 TeV, the cross sections for the Higgs boson production are improved by about 27%.

In Fig.1, we present the improved ResBos predictions of the transverse momentum distribution of Higgs boson produced by the gluon fusion, compared with the predictions of old ResBos (including only $C^{(1)}$) and HqT. The predictions of ResBos improved by including $C^{(2)}$ generally increase the overall size of the distribution. Especially, the improvement in the small transverse momentum region can be as large as 20% at both the Tevatron and LHC, and the peak position is slightly changed to the small Q_T region. Meanwhile the improved ResBos predictions are suppressed by about 20% for $Q_T \sim 60$ GeV (80 GeV) at the Tevatron (LHC). This behavior is due to the fact that the inclusion of NNLO Wilson coefficient functions can modify the matching procedure from resummed results to fixed-order ones when Q_T increases. The HqT predictions at the LHC for 7 TeV, 8 TeV and 14 TeV in small Q_T region are almost the same as the improved ResBos, but the peak height of the HqT prediction at the Tevatron is a little lower than that of the improved ResBos. However, the HqT predictions at large Q_T region is closer to the old ResBos predictions that include only $C^{(1)}$, and can be 20% higher than the improved ResBos predictions for $Q_T \sim 60$ GeV (80 GeV) at the Tevatron (LHC).

	m_H (GeV)	ResBos ($C^{(2)}$)	ResBos ($C^{(1)}$)	HNNLO (NNLO)	HqT (NNLL+NLO)
Tevatron	115	$0.98^{+9.2\%}_{-6.1\%}$	$0.91^{+15.7\%}_{-6.9\%}$	$0.96^{+13.6\%}_{-13.7\%}$	$0.97^{+14.2\%}_{-13.8\%}$
	120	$0.87^{+9.2\%}_{-6.9\%}$	$0.80^{+15.8\%}_{-6.6\%}$	$0.84^{+13.4\%}_{-13.7\%}$	$0.85^{+13.9\%}_{-13.8\%}$
	125	$0.77^{+9.1\%}_{-6.5\%}$	$0.71^{+15.9\%}_{-6.5\%}$	$0.75^{+13.5\%}_{-14.2\%}$	$0.75^{+13.8\%}_{-13.8\%}$
	130	$0.68^{+10.3\%}_{-5.9\%}$	$0.63^{+15.9\%}_{-6.4\%}$	$0.66^{+14.5\%}_{-13.1\%}$	$0.67^{+13.9\%}_{-13.8\%}$
LHC 7 TeV	115	$15.11^{+7.8\%}_{-5.8\%}$	$14.21^{+8.3\%}_{-5.9\%}$	$15.16^{+9.0\%}_{-10.7\%}$	$15.19^{+10.8\%}_{-10.4\%}$
	120	$13.89^{+7.8\%}_{-5.7\%}$	$13.06^{+8.4\%}_{-5.8\%}$	$13.80^{+10.6\%}_{-10.5\%}$	$13.94^{+10.2\%}_{-10.4\%}$
	125	$12.80^{+7.7\%}_{-5.5\%}$	$12.03^{+8.5\%}_{-5.6\%}$	$12.72^{+10.2\%}_{-10.6\%}$	$12.83^{+10.7\%}_{-10.4\%}$
	130	$11.83^{+7.7\%}_{-5.4\%}$	$11.12^{+8.6\%}_{-5.5\%}$	$11.75^{+10.8\%}_{-10.7\%}$	$11.84^{+9.9\%}_{-10.4\%}$
LHC 8 TeV	115	$19.15^{+7.5\%}_{-6.5\%}$	$17.58^{+8.1\%}_{-7.1\%}$	$19.05^{+9.9\%}_{-9.2\%}$	$19.25^{+10.8\%}_{-9.8\%}$
	120	$17.65^{+7.5\%}_{-6.5\%}$	$16.21^{+8.1\%}_{-7.1\%}$	$17.59^{+9.7\%}_{-9.9\%}$	$17.76^{+9.8\%}_{-10.1\%}$
	125	$16.31^{+7.5\%}_{-6.4\%}$	$14.98^{+8.1\%}_{-7.0\%}$	$16.26^{+10.2\%}_{-10.4\%}$	$16.39^{+9.8\%}_{-10.1\%}$
	130	$15.11^{+7.5\%}_{-6.4\%}$	$13.89^{+8.1\%}_{-7.0\%}$	$15.07^{+10.9\%}_{-10.6\%}$	$15.17^{+10.3\%}_{-10.1\%}$
LHC 14 TeV	115	$48.84^{+7.6\%}_{-5.7\%}$	$46.03^{+10.0\%}_{-5.3\%}$	$49.24^{+9.4\%}_{-9.8\%}$	$48.90^{+9.0\%}_{-9.8\%}$
	120	$45.45^{+7.5\%}_{-5.5\%}$	$42.84^{+9.8\%}_{-5.2\%}$	$45.57^{+10.4\%}_{-9.5\%}$	$45.52^{+10.3\%}_{-8.4\%}$
	125	$42.39^{+7.4\%}_{-5.4\%}$	$39.96^{+9.6\%}_{-5.0\%}$	$42.61^{+9.6\%}_{-9.7\%}$	$42.57^{+9.7\%}_{-8.8\%}$
	130	$39.65^{+7.3\%}_{-5.2\%}$	$37.38^{+9.4\%}_{-4.8\%}$	$39.93^{+11.1\%}_{-9.8\%}$	$39.75^{+9.7\%}_{-8.9\%}$

TABLE I: The ResBos, HNNLO and HqT theoretical predictions of the total cross sections (pb) for Higgs boson production $p + p \rightarrow H + X$ at the Tevatron (1.96 TeV) and LHC (7 TeV, 8 TeV and 14 TeV). The upper (lower) uncertainties expressed as percentages obtained by dividing (multiplying) the default scale by two.

Fig.2 shows the resummation scale dependence of the transverse momentum distribution of the Higgs boson in gluon fusion process at the Tevatron and LHC. To estimate the resummation scale dependence, we vary the hard scale coefficient C_2 by a factor of two around the canonical choice, but hold the relations between $C_{1,2,3,4}$ in Eq.(18). With this choice, the Wilson coefficient functions C_{gg} and C_{gq} do not change when C_2 is varied. Therefore, it is the shape of distributions that can be mainly affected by varying resummation scale. As shown in Fig.2, the shape of the transverse momentum distribution of Higgs boson is changed at both Tevatron and LHC. The peaks of the distribution are shifted by several GeV as varying the scales. Generally the distributions in the low and high Q_T regions are increased and suppressed, respectively, as increasing C_2 . The Q_T distributions for different scale choices cross at about 15 GeV. The main contribution in the low Q_T region, which dominates the total cross section, comes from the resummation piece, which is scale invariant after including enough high order contributions from A , B and C functions. The difference in the total cross sections originates mainly from the fixed-order contributions, which are matched with resummation piece to obtain the final distributions.

Fig.3 shows the ratios of the transverse momentum distributions between with and without G-functions at the Tevatron and LHC. It can be seen that the effect of G-functions is very small. As shown in figure, by including G-functions, the shape of transverse momentum distribution is slightly changed but the size is smaller than 1%. The reason is that for Higgs production process the lowest order where the G-function terms appear is NNLO without collinear singularities. The oscillation of ratio curves is due to numerical uncertainties.

Fig.4 presents the dependence on non-perturbative coefficients of the soft gluon resummation predictions on the transverse momentum distribution at the Tevatron and LHC. Based on the best-fit non-perturbative coefficients in BLNY parameterization [35] but scaled by a color factor ratio $C_A/C_F = 9/4$, the dependence on the non-perturbative coefficients is shown by multiplying or dividing the best-fit values by two. We can see that at both the Tevatron and LHC the peak position is shifted to larger Q_T and the peak height is decreased by a few percent at the Tevatron but hardly changed at the LHC when the non-perturbative coefficients increase. Moreover, when the non-perturbative coefficients are decreased the peak position is slightly moved to smaller Q_T , but the peak height remains the same. In the small $Q_T (< 4 \text{ GeV})$ region, the variation of non-perturbative coefficients can bring about 20% increment or decrement at most. In this region, the non-perturbative physics is dominant and may be used to probe the non-perturbative function form and coefficients. However, it will be difficult to obtain experiment data with small errors. Therefore, the peak position and height will be more efficient approaches to determine the non-perturbative coefficients for the processes with gluon initial states.

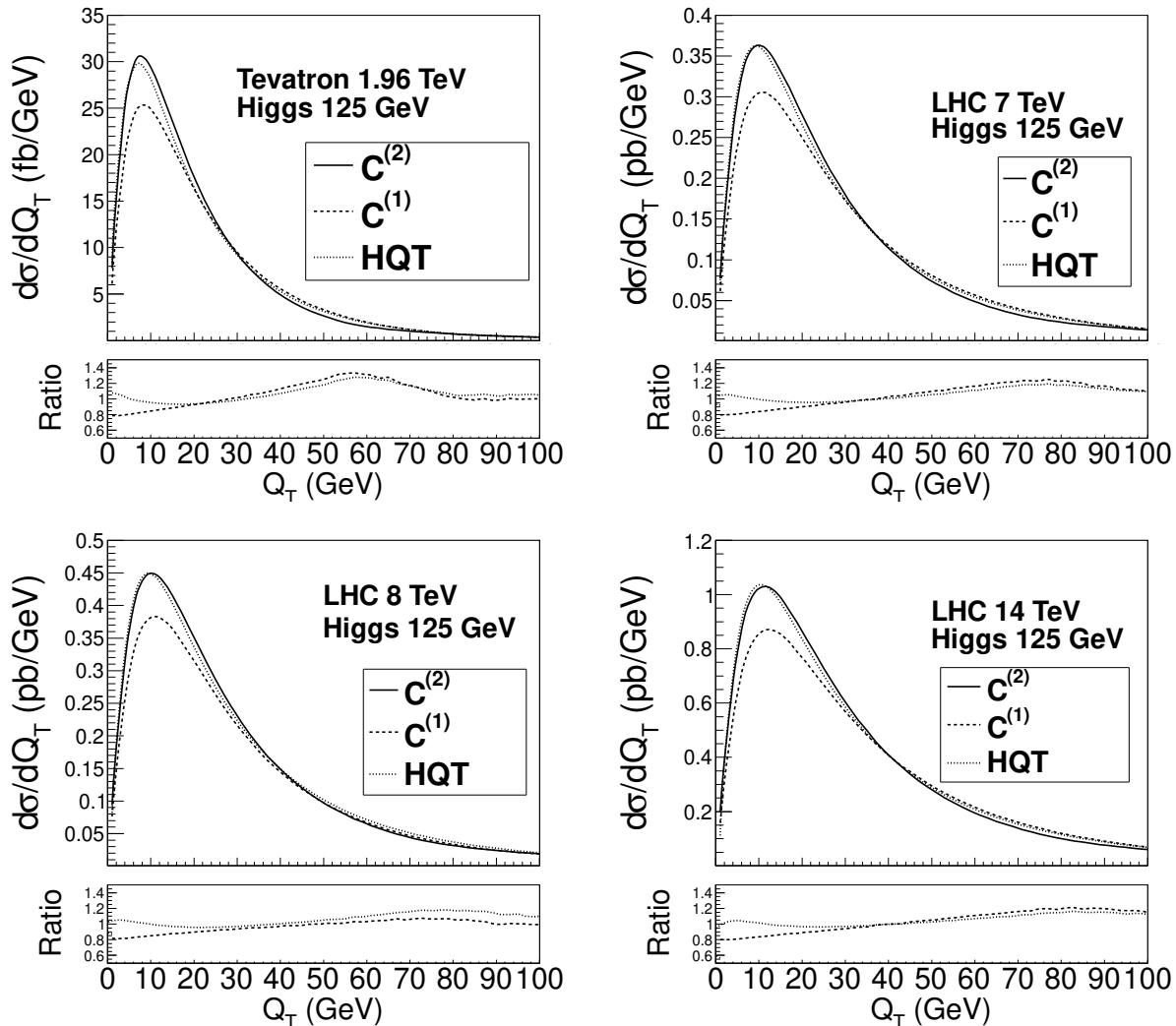


FIG. 1: The different theoretical predictions of the transverse momentum distribution for the Higgs boson production at the Tevatron (1.96 TeV) and LHC (7 TeV, 8 TeV and 14 TeV). In the bottom of each plot, the ratios to improved ResBos predictions are also shown.

IV. CONCLUSION

In conclusion, we have improved the resummation formula in ResBos for the Higgs boson production by including the NNLO Wilson coefficient functions and G-functions. We show that the improvement from NNLO Wilson coefficient functions increases the total cross section prediction of ResBos for Higgs production by about 8% at the Tevatron and about 6% at the LHC. And we find that the NNLO prediction of HNNLO and NNLL+NLO prediction of HqT are consistent with improved ResBos prediction within a couple of percents at the Tevatron and LHC. Also, we show that for the transverse momentum distribution, the improved predictions of ResBos generally increase the overall size of the distribution. Especially, the improvement in the small transverse momentum region can be as large as 20% at both the Tevatron and LHC, but the peak position is not changed. The HqT predictions for the transverse momentum distribution at the LHC are almost the same as the improved ResBos, except that the peak height of the HqT prediction at the Tevatron is a little lower than of the improved ResBos. Moreover, the distributions in the low and high Q_T regions are increased and suppressed, respectively, as increasing the renormalization constant C_2 and keeping the relations between $C_{1,2,3,4}$. The G-functions has little effect on the transverse momentum distribution, which can only modify the distribution shape within 1%. Besides, varying the non-perturbative coefficients by a factor of two can slightly change the peak position and height of the distribution.

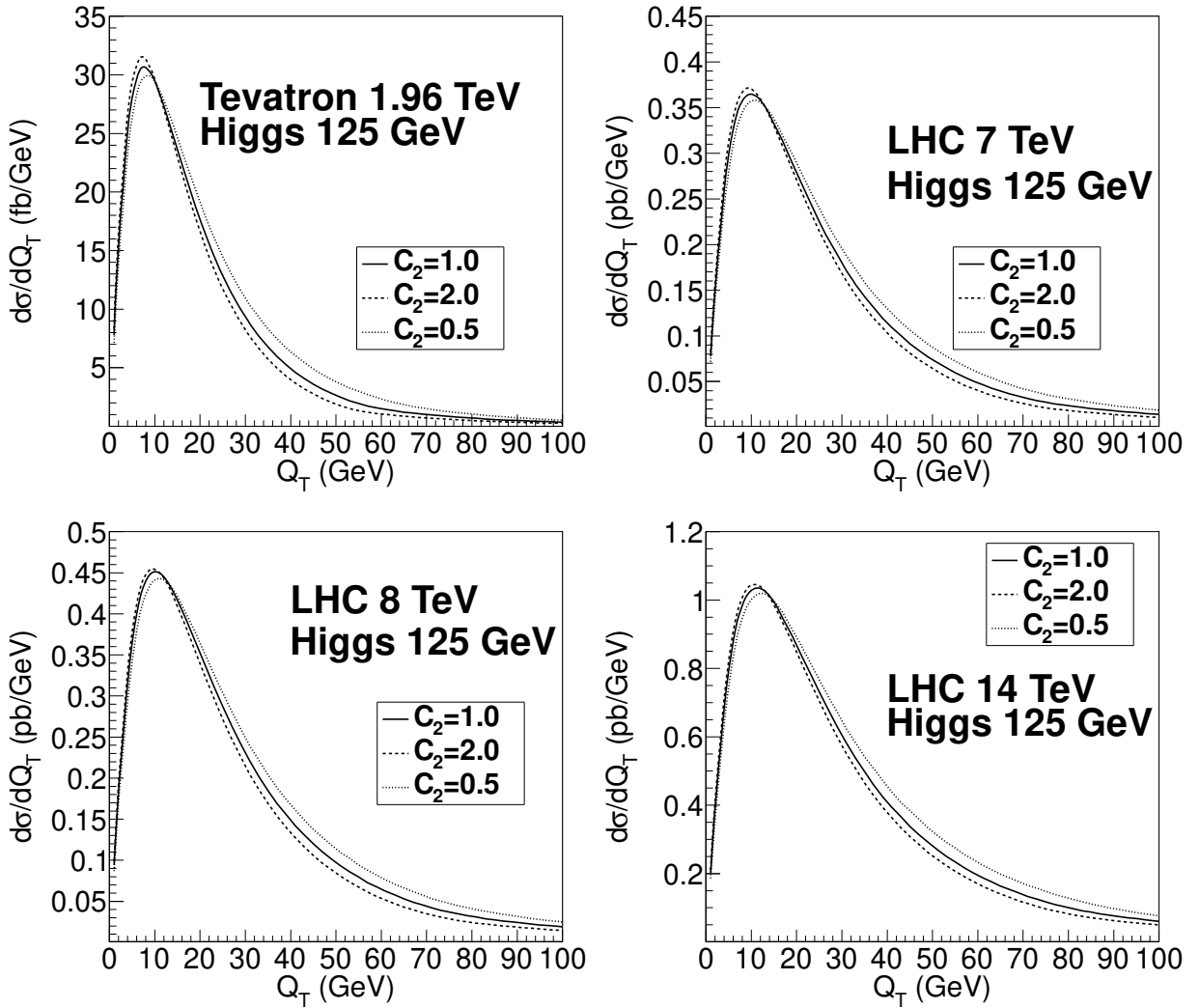


FIG. 2: The transverse momentum distributions for different scale choices at the Tevatron (1.96 TeV) and LHC (7 TeV, 8 TeV and 14 TeV).

Acknowledgments

Jian Wang, Chong Sheng Li, and Hai Tao Li were supported by the National Natural Science Foundation of China, under Grants No. 11021092 and No. 10975004. Zhao Li and C.-P. Yuan were supported by the U.S. National Science Foundation under Grant No. PHY-0855561.

-
- [1] Report FERMILAB-CONF-12-065-E, CDF Note 10806, D0 Note 6303 (2012).
[2] Report CERN-PH-EP-2012-019 (2012), 1202.1408.
[3] S. Chatrchyan et al. (CMS Collaboration) (2012), 1202.1488.
[4] S. Dawson, Nucl.Phys. **B359**, 283 (1991).
[5] A. Djouadi, M. Spira, and P. Zerwas, Phys.Lett. **B264**, 440 (1991).
[6] D. Graudenz, M. Spira, and P. Zerwas, Phys.Rev.Lett. **70**, 1372 (1993).
[7] M. Spira, A. Djouadi, D. Graudenz, and P. Zerwas, Nucl.Phys. **B453**, 17 (1995), hep-ph/9504378.
[8] R. V. Harlander and W. B. Kilgore, Phys.Rev.Lett. **88**, 201801 (2002), hep-ph/0201206.
[9] C. Anastasiou and K. Melnikov, Nucl.Phys. **B646**, 220 (2002), hep-ph/0207004.
[10] V. Ravindran, J. Smith, and W. L. van Neerven, Nucl.Phys. **B665**, 325 (2003), hep-ph/0302135.

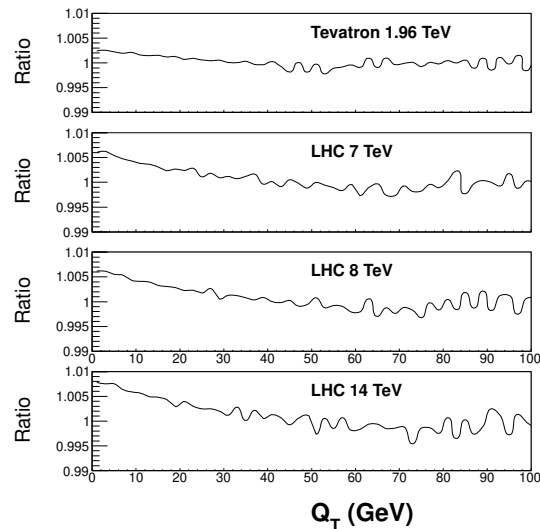


FIG. 3: The ratios of the transverse momentum distributions between with and without G-functions at the Tevatron (1.96 TeV) and LHC (7 TeV, 8 TeV and 14 TeV).

- [11] S. Marzani, R. D. Ball, V. Del Duca, S. Forte, and A. Vicini, Nucl.Phys. **B800**, 127 (2008), 0801.2544.
- [12] R. V. Harlander and K. J. Ozeren, JHEP **0911**, 088 (2009), 0909.3420.
- [13] A. Pak, M. Rogal, and M. Steinhauser, Phys.Lett. **B679**, 473 (2009), 0907.2998.
- [14] S. Catani, D. de Florian, M. Grazzini, and P. Nason, JHEP **0307**, 028 (2003), hep-ph/0306211.
- [15] V. Ahrens, T. Becher, M. Neubert, and L. L. Yang, Phys.Rev. **D79**, 033013 (2009), 0808.3008.
- [16] V. Ahrens, T. Becher, M. Neubert, and L. L. Yang, Eur.Phys.J. **C62**, 333 (2009), 0809.4283.
- [17] V. Ravindran, J. Smith, and W. Van Neerven, Nucl.Phys. **B634**, 247 (2002), hep-ph/0201114.
- [18] C. J. Glosser and C. R. Schmidt, JHEP **0212**, 016 (2002), hep-ph/0209248.
- [19] C. Anastasiou, K. Melnikov, and F. Petriello, Nucl.Phys. **B724**, 197 (2005), hep-ph/0501130.
- [20] S. Catani and M. Grazzini, Phys.Rev.Lett. **98**, 222002 (2007), hep-ph/0703012.
- [21] M. Grazzini, JHEP **0802**, 043 (2008), 0801.3232.
- [22] J. M. Campbell, R. K. Ellis, and G. Zanderighi, JHEP **0610**, 028 (2006), hep-ph/0608194.
- [23] G. Bozzi, S. Catani, D. de Florian, and M. Grazzini, Phys.Lett. **B564**, 65 (2003), hep-ph/0302104.
- [24] G. Bozzi, S. Catani, D. de Florian, and M. Grazzini, Nucl.Phys. **B737**, 73 (2006), hep-ph/0508068.
- [25] G. Bozzi, S. Catani, D. de Florian, and M. Grazzini, Nucl.Phys. **B791**, 1 (2008), this paper is dedicated to the memory of Jiro Kodaira, great friend and distinguished colleague, 0705.3887.
- [26] D. de Florian, G. Ferrera, M. Grazzini, and D. Tommasini, JHEP **1111**, 064 (2011), 1109.2109.
- [27] T. Becher and M. Neubert (2012), 1205.3806.
- [28] C. Balazs and C. P. Yuan, Phys. Rev. **D56**, 5558 (1997), hep-ph/9704258.
- [29] J. C. Collins and D. E. Soper, Nucl.Phys. **B193**, 381 (1981).
- [30] J. C. Collins and D. E. Soper, Nucl.Phys. **B197**, 446 (1982).
- [31] J. C. Collins, D. E. Soper, and G. F. Sterman, Nucl.Phys. **B250**, 199 (1985).
- [32] Q.-H. Cao, C.-R. Chen, C. Schmidt, and C.-P. Yuan (2009), 0909.2305.
- [33] C. Balazs and C. Yuan, Phys.Lett. **B478**, 192 (2000), hep-ph/0001103.
- [34] M. Kramer, E. Laenen, and M. Spira, Nucl.Phys. **B511**, 523 (1998), hep-ph/9611272.
- [35] F. Landry, R. Brock, P. M. Nadolsky, and C. Yuan, Phys.Rev. **D67**, 073016 (2003), hep-ph/0212159.
- [36] S. Catani and M. Grazzini (2011), 1106.4652.
- [37] S. Catani and M. Grazzini, Nucl.Phys. **B845**, 297 (2011), 1011.3918.
- [38] P. M. Nadolsky et al., Phys. Rev. **D78**, 013004 (2008), 0802.0007.

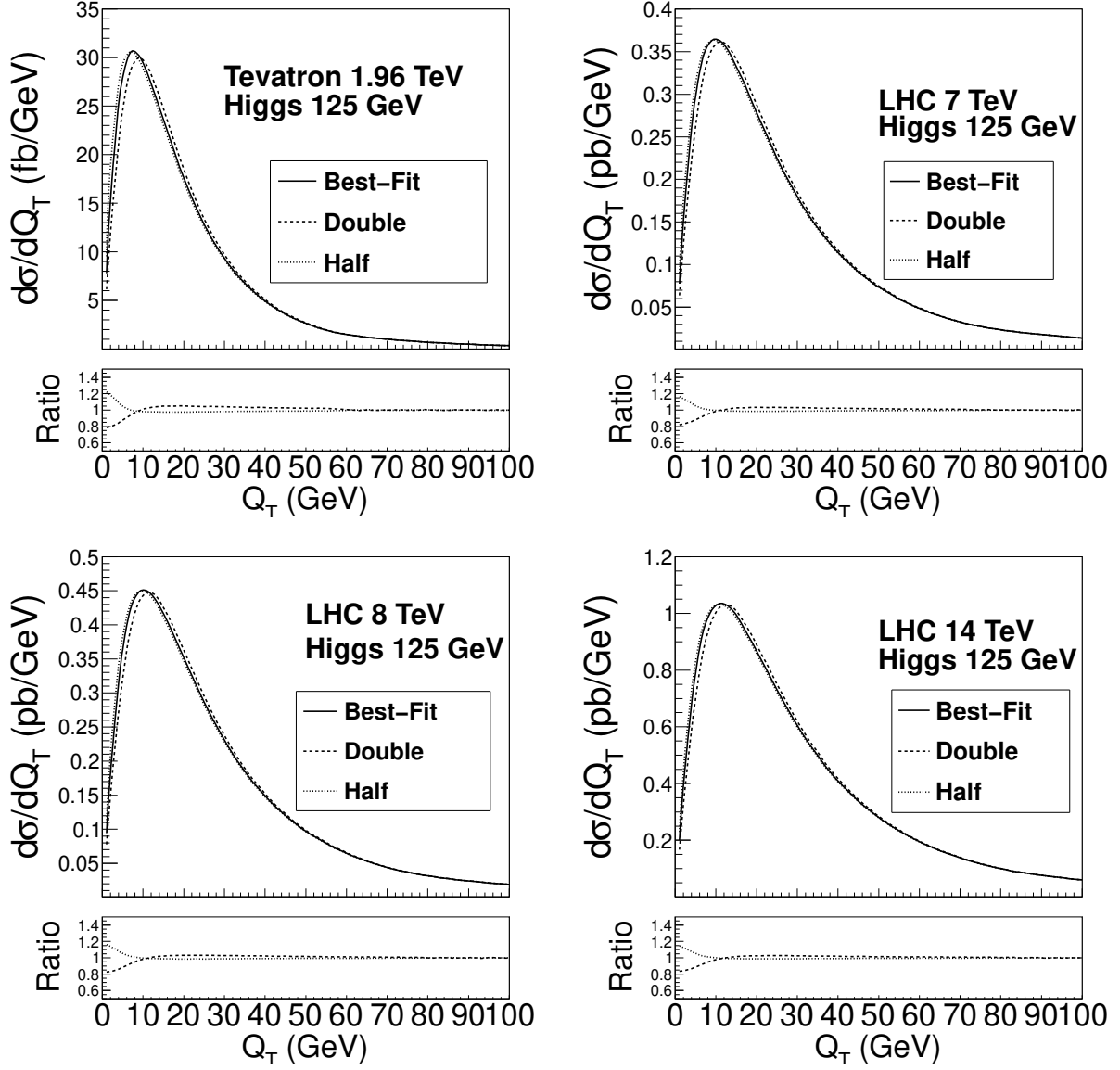


FIG. 4: The transverse momentum distribution for different non-perturbative parameter choices at the Tevatron (1.96 TeV) and LHC (7 TeV, 8 TeV and 14 TeV).